A COMPREHENSIVE COMPARISON AMONG CLASSICAL AND GOODING METHODS OF INITIAL ORBIT DETERMINATION IN OPTIMIZED ELECTRO- OPTICAL SENSOR NETWORKS

C. A. Miller and C. Frueh

Purdue University School of Aeronautics and Astronautics, West Lafayette, IN, USA, Email: {mill1955, cfrueh}@purdue.edu

ABSTRACT

Since Gauss invented the first initial orbit determination method, a multitude of methods exist to determine an orbit of a set of assocuated measurements. Each method has particular strengths, however, they are sometimes not easily gauged from the method itself, especially in the presence of measurement noise. In this paper, a ground-based optical sensor is asssumed. The goal of this paper is to comprehensively compare a classical initial orbit determination method, in this case Gauss's original method, with that of a more modern one, classical Gooding's method and the Gooding method in using Der's algorithm to solve the Lambert problem. The effects of spacing are characterized in dependence of both short and multi-revolution arcs, measurement noise, changes in observer latitude, semi-major axis, and eccentricity.

Keywords: Initial Orbit Determination; Gauss; Gooding; Electro-Optical.

1. INTRODUCTION

Initial orbit determination (IOD) is the process of taking measurements of a resident space object (RSO) and using those to determine a preliminary estimate of the object's orbit[4]. There are a variety of methods tailored to different sensors like, doppler, laser-ranging, and radar which measure different subsets of the six parameter space of position and velocity[3]. Optical ground-based telescopes are a cost efficient sensor for observations on high altitude orbits especially. Initial orbit determination from optical observations, otherwise known as angles-only IOD, relies upon three measurements consisting of the epoch, and two angles[9]. After acquisition, the measurements may be fed into a variety of available algorithms in order to determine the initial orbit.

These IOD algorithms are a large topic of research with a multitude of methods available. The classical methods are Laplace and Gauss, while more recently there are, e.g., Escobal's double-R and Gooding's method[12][13]. Gauss's method relies upon the planar geometry of standard Keplerian motion while Gooding relies on range iteration for its estimate. These methods, despite using different solvers at their core, are both deterministic and assume that the input measurements are perfect. While there has been significant work on making statistical orbit determination methods [1], statistical Lambert solvers [17], and augmenting existing methods to account for uncertainties [2], there is a need to characterize the susceptibility of available methods like Gauss and Gooding to measurement error and the measurement geometry.

The effect of measurement error on IOD has been previously studied in detail for the Herrick-Gibbs method, which is not an optical method, where a solution to mitigate these effects was proposed and analyzed [20]. Below one revolution, in general state error with the presence of noise tends to decrease as the spacing increases [5]. Above one full revolution, error tends to increase drastically for many IOD methods as there is indeterminancy between mutliple possible solutions. Many solutions to these multiple revolution cases have been proposed such as trial and error of different arcs across multiple revolutions while trying to match the time of flight [8] or by using pairs of user-specified variables in analytic equations to solve for the state [15]. As such, there is a trade-off between the measurement error and the measurement spacing for a given method, but also between different methods. As such, it is relevant for sensor tasking to have an understanding of the optimal measurement spacing for a given sensor or sensor network and expectet error profile [10][11].

In the following, Gauss and Goodings method will briefly be introduced, followed by an introduction of a modified Gooding method, called Gooding-Der method. The methods are tested under various observer latitudes, measurement errors and measurement spacing and comprehensively analysed. The paper concludes with a summary of the findings.

2. GAUSS'S METHOD

Gauss's method is based around Keplerian orbits being planar, observations may not all be in the same plane, but the positions of satellite are:

$$c_1\mathbf{r_1} + c_2\mathbf{r_2} + c_3\mathbf{r_3} = 0 \tag{1}$$

The algorithm also necessitates ten triple products created from the lines-of-sight, L_i, and the station vectors, $R_{stat,i}$ for each measurement where one of them, D_0, serves as the denominator in calculations of multiple quantities:

$$D_0 = \mathbf{L_1} \cdot (\mathbf{L_2} \times \mathbf{L_3}) \tag{2}$$

This singularity created from using this quantity in the denominator becomes evident when considering observations made all in the same plane. For example, take a near equatorial station vector measuring a space object at 0°inclination, this quantity will become zero resulting in a singularity for this entire scenario.

Additionally, Gauss's method requires solving the roots of an eighth order polynomial for the magnitude of the position of the space object for measurement two:

$$||\mathbf{r_2}||^8 + a||\mathbf{r_2}||^6 + b||\mathbf{r_2}||^3 + c = 0 \tag{3}$$

This polynomial will necessarily yield eight roots, of which the imaginary and negative roots are discarded. In most cases, this leaves only one viable root but occasionally there remain two. Without other a priori knowledge, it is impossible to distinguish between the two roots in terms of which one is closer to the correct solution. Though some work has been done in selecting between viable roots [21], this ambiguity is inherent to Gauss's method amd for the purposes of this paper if this situation was encountered, the smallest of the viable roots is chosen as the solution arbitrarily.

3. GOODING'S METHOD

Gooding's method is that of range iteration, taking a guess-and-check approach to IOD [6]. It starts off with some set of initial guesses for the range such that two full position vector guesses for the target may be created:

$$\mathbf{r_i} = \mathbf{R_{stat,i}} + \rho_i \mathbf{L_i} \tag{4}$$

A Lambert solver [14] can then be called, using the time between the two corresponding measurements:

$$[\mathbf{v_i}, \mathbf{v_j}] = Lambert(\mathbf{r_i}, \mathbf{r_j}, t_j - t_i) \tag{5}$$

The method then propagates the state generated by the Lambert solver to the time of the as yet unused measurement. It then compares the angular offset of the estimated and true measurement via a dot product. If this dot product is nearly one then the method has converged to a solution. Where the unit vector line of sight of the estimated position is $L_{i,est}$ and the truth is L_i, the residual to be minimized is:

$$f = 1 - \mathbf{L_{i,est}} \cdot \mathbf{L_i} \tag{6}$$

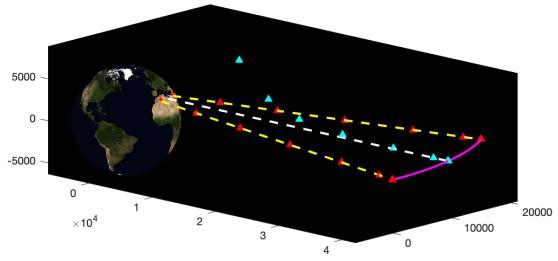

Figure 1. Cartesian plot showing the measure lines-of-sight with L_1 and L_3 in yellow and L_2, the truth for the residual, in white. Range guesses are shown for each iteration in red triangles, and the converging range estimate for L_2 is shown in cyan trangles. The truth orbit is shown as an arc in magenta.

The algorithm must then figure out in what direction it should update the ranges for the guesses and with what magnitude. Gooding does this by slightly perturbing the ranges methodically up and down from the starting guess of the iteration in order to get a numerical derivative of the error with respect to a change in the range guesses. This must be done five times given that this is a bivariate problem: increasing and then decreasing the first range guess, then the second range guess, then either increasing or decreasing both simultaneously. Then a bivariate Newton-Raphson method is performed with this derivative information in order to update the range guesses for the next iteration.

It should be noted that in Gooding's formulation, it is chosen to give range guesses to the first and third measurements, leaving the second measurement as the truth which to compare the estimated solution. While the programs created in support of this paper adhere to this structure, any combination of these pairings will likely produce valid results and any differences would be down

to the propagation time and accuracy of the propagator from one state to another. The initial guesses given to the Gooding method for all cases in this paper are one Earth radius.

Given that the Lambert solver is crucial to the convergence of the method and the determination of a state estimate, other Lambert solvers were also investigated. Of particular interest is a Lambert solver based on universal variables [7] and then modified to to check a number of possible orbits greater than one full revolution [8].

4. GOODING-DER'S METHOD

Since on crucial part of Gooding's method is its Lambert solver, a clear avenue for improvement is to replace its original Lambert solver with a better one. Der's Lambert solver improves on Gooding's in two key ways: it uses Sun's universal variables to converge on velocity solutions even with arcs spanning multiple revolutions as well as using the Laguerre algorithm, a higher order iterative solver to solve the Lambert equation.

Lambert's equation for elliptic multi-revolution arcs:

$$F(x) = f(x) - f(y) + N\pi - g(x)\tau \tag{7}$$

Then according to Sun [7] and Der [8] elliptic orbits span $-1 < x < 1$, parabolic orbits have $x = 1$ and hyperbolic orbits have $x > 1$. Specifically for elliptic orbits if $-1 < x < 0$ the orbit is the high path, if $x = 0$ then the trajectory is the minimum energy path, and finally, if $0 < x < 1$ then the trajectory is the low path.

Relating back to the standard Kepler problem, x, y, and σ are given by:

$$x^2 = 1 - \frac{m}{4a} \tag{8}$$

$$y^2 = 1 - \frac{n}{4a} \tag{9}$$

$$\sigma^2 = \frac{1 - y^2}{1 - x^2} \tag{10}$$

Where m is the perimeter of the Lambert triangle, $n = r_1 + r_2 - c$, $c = |\mathbf{r_1} - \mathbf{r_2}|$, and a is the semi-major axis [8].

5. NUMERICAL SIMULATION SETUP

In order to compare the three methods of initial orbit determination of interest in this paper, a viable set of test cases must be found which are representative of the typical satellite for which these algorithms will be run.

For the orbit, two parameters of interest are semi-major axis and eccentricity, as parameters which are prone to misrepresentation in an IOD method and also lead to severe effects when determined far off from the truth, as the object will not be re-observed in follow-up observations.

Of particular interest is the effect of the ground-based observer position and the measurement spacing in the presence of measurement noise on the initial orbit determination. The parameter space of the observer position scenario allows for the variation of altidude, latitude, and longitude when limited to Earth-based observers. Altitude was ruled out as a parameter of interest as the effect of feasible altitudes, as compared to the Earth's radius, is negligible on IOD, especially with respect to the othereffects. For a geosynchronous object, the effect of longitude is less interesting, as it is equal to a change in anomaly and is hence not explored here. To explore the observer latitude effects, the angle between observations is varying between 0.0573°and 181.8°in true anomaly of the respective orbit with 20 linearly spaced increments and the latitude was varied between 0°and 90°with 10 linearly spaced increments.

Finally, the measurement spacing is crucial. In the first set of cases, eccentricity and spacing has been varied, with the spacing varying between 1 minute and 600 minutes with 20 linearly spaced increments, while eccentricity was varied between 0 and 0.95 in 10 linearly spaced increments. For the semi-major axis vs. spacing, the measurement spacing was varied between 0.0573°and 181.8°in true anomaly of the respective orbit with 20 linearly spaced increments and the semi-major axis was varied between 6778 km and 42'000km in 10 linearly spaced increments.

For the measurement noise, a noise of zero, 1 arcsecond and 10 arcseconds has been assumed for all cases.

5.1. Scenario Statistics

Table 1. Orbit parameters for eccentricity vs spacing case and observer location at first measurement. True anomaly is also given at first measurement.

Parameters	Value
Perigee Radius	42164
Eccentricity	Variable
Inclination	0°
RAAN	Undefined
True Anomaly	180°
Observer Latitude	30°
Observer Longitude	Obs. Long. = RSO Long.

Table 2. Semi-major axis vs spacing case orbital parameters. Observer parameters and true anomaly are only for first observation.

Parameters	Value
Perigee Radius	Variable
Eccentricity	0
Inclination	0°
RAAN	Undefined
True Anomaly	180°
Observer Latitude	30°
Observer Longitude	Obs. Long. = RSO Long.

Table 3. Observer latitude vs. spacing scenario, orbital parameters and observer location as well as true anomaly at first observation.

Parameters	Value
Perigee Radius	42164
Eccentricity	0
Inclination	0°
RAAN	Undefined
True Anomaly	180°
Observer Latitude	Variable
Observer Longitude	Obs. Long. = RSO Long.

6. RESULTS

6.1. Varying Eccentricity

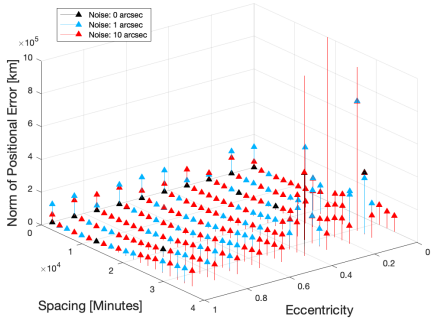

Figure 2. Gauss's positional error when changing eccentricity and spacing(1).

Gauss's method shows a relatively smooth increase in positional error as the spacing increases. Like with other methods, too-short arcs are apparent even with the smallest even second-smallest spacing, increasing the positional error. Eccentricity appears to only produce large differences in area for large spacings, especially between eccentricities of 0.1 and 0.3.

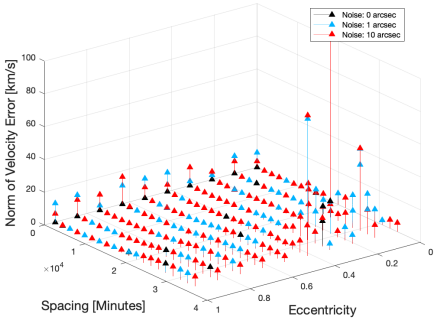

Figure 3. Magnitude of velocity error for Gauss's method while changing spacing of observations vs. eccentricity (1).

The velocity error of Gauss's method shows similar trends to that of its positional error; however the differences between the low error and high error are reduced for velocity. This indicates that Gauss provides more stable velocity estimates than positional estimates under this set of scenarios.

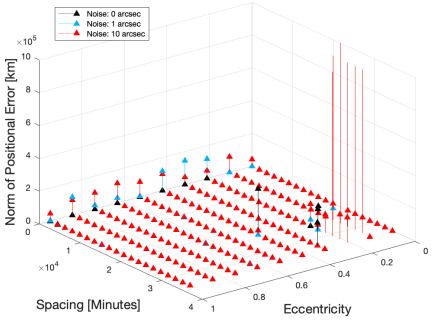

Figure 4. Norm of positional error for Gooding's method for changing spacing and eccentricity (1).

For the position estimates, Gooding follows similar trends to that of Gauss with the too-short arc singularity and instability for e = 0.1 to e = 0.3. Despite, these similarities the error in position in much lower than that of Gauss.

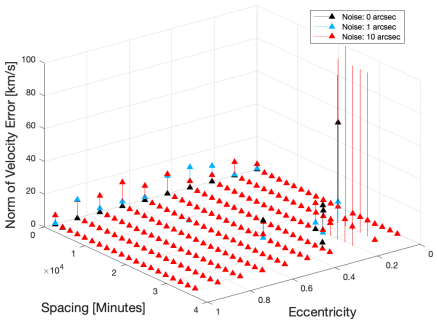

Figure 5. Magnitude of velocity error for Gooding's method with changes in spacing and eccentricity. (1).

Gooding's error in the velocity estimate with changing eccentricity has similarly low error to its positional estimate and does not rise appreciably along with spacing.

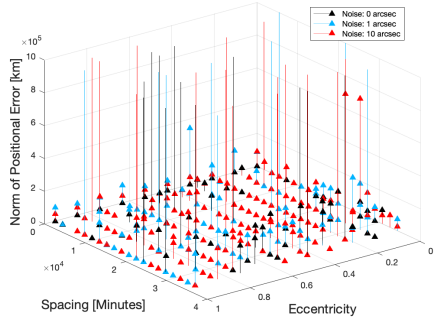

Figure 6. Norm of positional error for Gooding-Der's method for changing spacing and eccentricity (1).

Fig. 6 shows that Gooding-Der's method for a range of eccentiricities and spacings is inconsistent in positional error. There is a region of low error at lower eccentricities and smaller spacings but as compared to Gooding's original method, Gooding-Der's is nearly unusable.

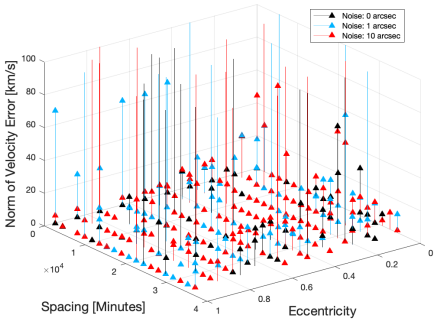

Figure 7. Magnitude of velocity error for Gooding-Der's method with changes in spacing and eccentricity. (1).

The velocity error of Gooding-Der in fig. 7 shows the same trends as the positional error: it is equally unreliable for velocity.

Gauss and Gooding, for the variety of cases involving changing eccentricity and measurement spacing, follow similar trends in both position and velocity error. Both methods show a singularity with large measurement spacing of around 550 to 600 minutes with an eccentriciy of around 0.2. The magnitude of positional error is overall lower with Gooding than with Gauss and is only magnified in the velocity error, where overall and especially for larger spacing, the error of Gauss goes up significantly while that of Gooding remains around zero.

6.2. Varying Semi-Major Axis

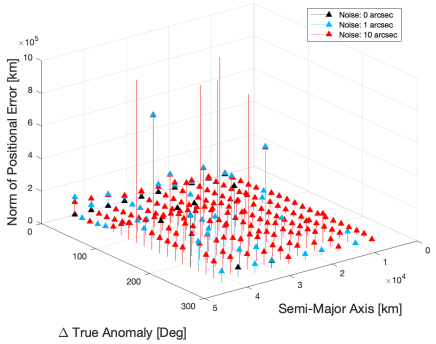

Figure 8. Changing semi-major axis and spacing case showing error in Gauss's method (2).

From fig. 8 it is shown that Gauss's positional estimate error increases with increasing semi-major axis and measurement spacing in a circular orbit and quickly becomes unstable.

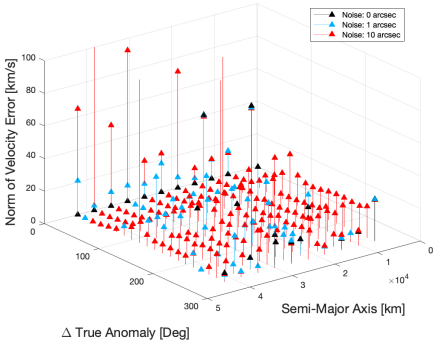

Figure 9. Velocity error for Gauss's method while changing spacing of observations vs. semi-major axis (2).

Unlike in fig. 2 and fig. 3 where the position and velocity estimates of Gauss show similar trends, 8 and fig. 9

differ significantly in their trends, showing the for changing semi-major axis, Gauss's velocity estimates are less stable.

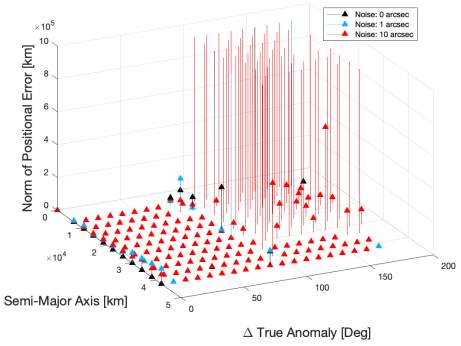

Figure 10. Positional error for Gooding's method in changing spacing and semi-major axes cases (2).

Gooding's estimate for changing semi-major axes are the least stable for both position as shown in fig. 10 and velocity as shown in the next figure. Positional error remains low for for high semi-major axis and low spacing but there is a sudden drop in stability upon reaching semi-major axis of less than around 40,000 km and spacings less than 100°apart.

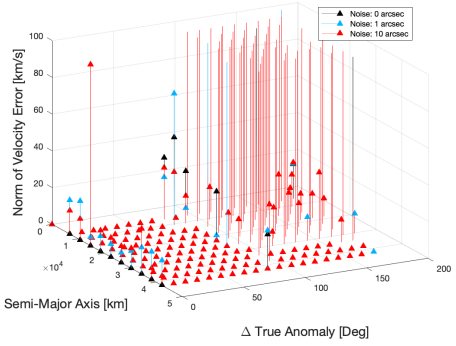

Figure 11. Velocity error for Gooding's method for changies in spacing and semi-major axis (2).

Fig. 11 shows a similarly drastic change in velocity error estimates as that fig. 8 in the same region. Error of the estimates outside of this region remain low except for the lowest spacing cases were too-short arcs come in again.

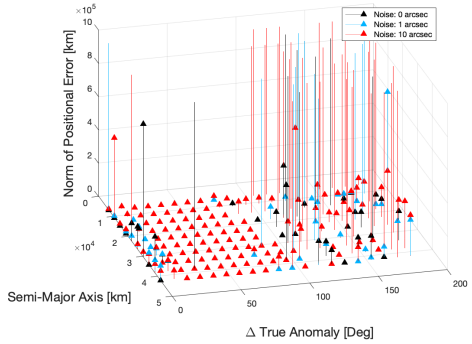

Figure 12. Positional error for Gooding-Der's method in changing spacing and semi-major axes cases (2).

Gooding-Der's and Gooding's method show similar drastic positional error increases with true anomalies above 90°as shown in fig. 12. Gooding-Der differs from Gooding in semi-major axes above that of geostationary where Gooding provides better estimates than Gooding-Der.

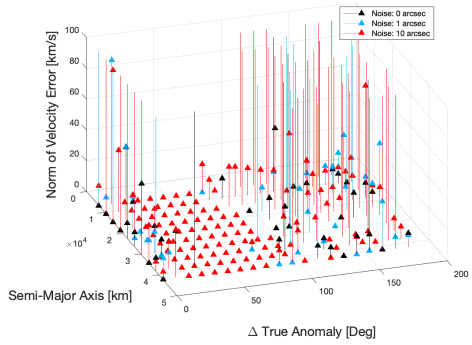

Figure 13. Velocity error for Gooding-Der's method for changies in spacing and semi-major axis (2).

The velocity estimate of Gooding-Der shows the same trends as its positional error however the realtive magnitudes in fig 13 are larger than for positional error, especially with low spacing between the measurements.

Focusing on the changing semi-major axis results, Gooding displays large indeterminancy below geostationary orbit and with spacings corresponding to a true anomaly above 90°. Gooding-Der shows similar instability with true anomaly though without the stability above geostationary. It has been noted before that such instability in circular orbits with larger measurement spacing is typical of Gooding's method [16] thus would likely affect Gooding-Der as well. Outside of this region, error in both position and velocity remain small until too-short arcs with noise come into play with small spacings. Meanwhile, Gauss's method in this unstable region offers greater positional accuracy as well as velocity accuracy, however the velocity error of Gauss in this region is still quite high. Gooding-Der differs from the previous two

methods and proves to be unreliable in producing low-error solutions for many of the tested cases.

6.3. Varying Observer Latitude

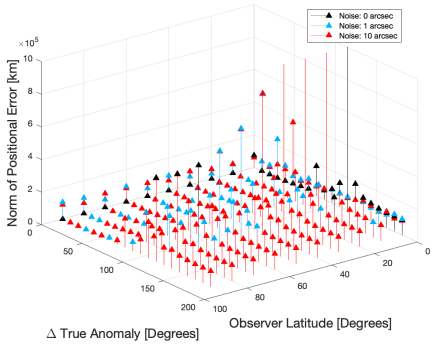

Figure 14. Magnitude of positional error for Gauss's method while changing spacing of observations and observer position(3).

Gauss's method shows a unique behavior for the changing observer latitude vs. spacing cases in fig. 14. Outside of the too-short arc region, positional error starts low, rising with spacing until a peak of instability at 90°, lowering but not returnig to the similarly low levels at the some of the lower spacings. The peak at 90°spacing is due to the ambiguity of the geometry, for a circular geostationary orbit with a measurement are spanning half of a full orbit, there are multiple solutions that are feasible.

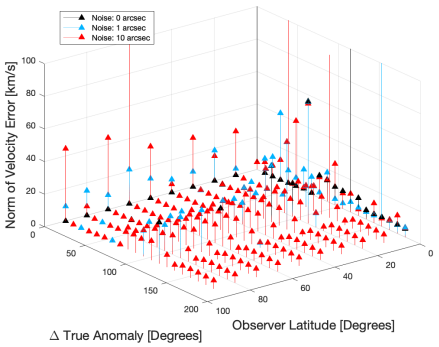

Figure 15. Norm of velocity error for Gauss's method while changing measurement spacing and observer latitude(3).

Fig. 15 shows similar trends, though less in magnitude, to that of fig. 11. Additionally it is shown that even with no noise, coplanar lines-of-sight greatly increase the error in both the position and velocity estimates due to the geometric indeterminancy of such cases.

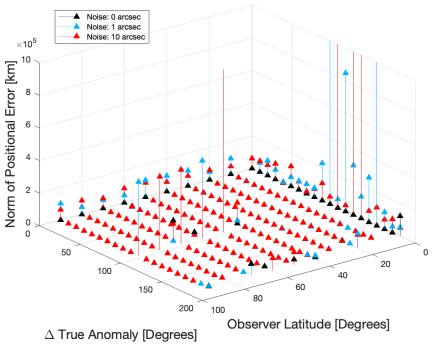

Figure 16. Positional error for Gooding's method with changing spacing and observer latitude(3).

Fig. 16 shows similar trends to that Gauss's position estimates for the observer latitude vs. spacing cases although the error for much of the series of cases is lower than that Gauss. The effect of indeterminacies is more abrupt in Gooding's method, a positive given that cases near such scenarios show less error than those of Gauss.

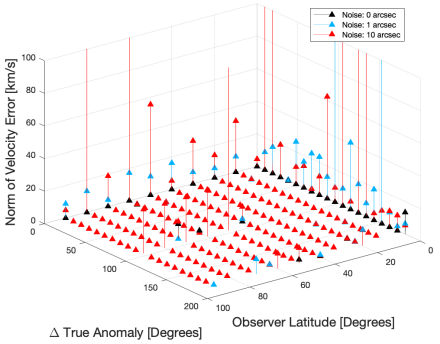

Figure 17. Observer latitude vs. spacing: velocity error of Gooding's method (3).

Fig. 17 shows the velocity estimate error of Gooding for the observer latitude vs. spacing cases. It shows similar trends to the position error, and, to a lesser magnitude, Gauss's velocity error. An interesting distinction between these estimates of Gauss and Gooding is for the the co-planar observer and orbit, the no noise scenario shows nearly zero error using Gooding's method but has significant error from Gauss's method. This follows similar results for Gooding where observer placement even in space-based IOD did not produce very different results using Gooding's method [19].

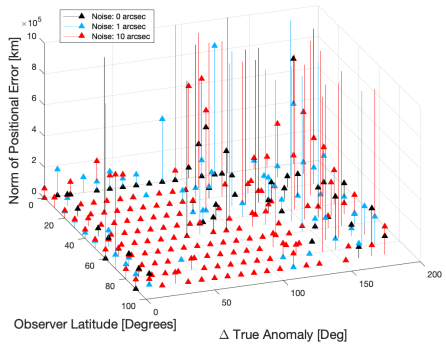

Figure 18. Positional error for Gooding-Der's method with changing spacing and observer latitude(3).

Fig. 18 follows the trends of the semi-major axis changing case where below a measurement arc spanning spanning half an orbit, the positional error remains low for all levels of noise, but behaves erratically above this threshold. Similar to other observer latitude cases, the error increases when coplanar measurements are used.

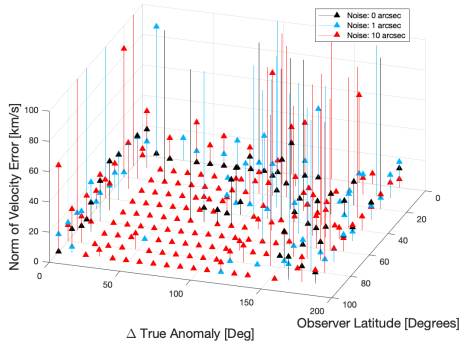

Figure 19. Observer latitude vs. spacing: velocity error of Gooding-Der's method (3).

Fig. 19 is shows behavior of the velocity error similar to that of Gooding-Der's positional error though with increased magnitude around the singularities.

Gooding's method and Gauss's show especially similar trends in this scenario. Both have a singulary at around 90°true anomaly change between each measurement they also show not only high error with small spacing between measurements but also high error with observer latitudes of 0°. This is due to the fact that in those cases, the observer and therefore the lines-of-sight lie in the same plane as the orbit. Additionally, the error due to those singularities has a much more abrupt jump with Gooding than with Gauss, adding to merit of Gooding. Additionally, numerical results for the minimum, median, and maximum position (4) and velocity (5) error are given in the appendix. Gooding-Der shows instabilities for over half of the cases in this regime, specifically when true anomaly between measurements grows above 70°. Overall across both the positional and velocity error Gooding has much higher accuracy than Gauss and Gooding-Der.

7. CONCLUSIONS

In short, Gooding's method in its classical formulation, as shown throughout the various test cases, is more accurate in the presence of measurement noise of a ground-based optical observer with a variety of different measurement spacings when comparing in both positional amf velocity error in state estimates of simulated orbits compared to both alternatives, Gauss and Gooding-Der. Gauss and Gooding show similar trends in the error when varying eccentricity and observer latitude but show very different trends when changing semi-major axis for circular, equatorial orbits. Gooding-Der deviates from both of these methods. The best case scenarios for Gooding's method are when the spacing between measurements represents less than a quarter of the target's orbit but is still greater than 5°.

Orbit determination of objects on highly eccentric pose challenges also in characterizing errors, as the measurement geometry is affected by the orientation of the orbit in the orbital plane. In the investigated cases, except for large spacings on the order of 8 to 10 hours for eccentricities of 0.1 to 0.3 where there is an indeterminancy in both methods, classical Gooding still provides the smallest error. Classical Gooding performs best with a measurement spacing of around one hour.

The Gooding-Der mothod unfortunately has proven to be inconsistent in its error profile.

REFERENCES

1. Armellin, R., Di Lizia, P. (2016). Probabilistic Initial Orbit Determination. *26th AAS/AIAA Space Flight Mechanics Meeting*
2. Armellin, R., Di Lizia, P., Lavagna, M., (2012). High-Order Expansion of the Solution of Preliminary Orbit Determination Problem. *Celestial Mechanics and Dynanical Astronomy* **112**, 331–352
3. Bate, R., Mueller, D., White, J., (1971). *Fundamentals of Astrodynamics*, Dover, ed. 1
4. Curtis, H., (2005). *Orbital Mechanics for Engineering Students*, Elsevier, ed. 1
5. Celletti, A., Pinzari, G. (2006). Dependence on the observational time intervals and domain of convergence of orbital determination methods. *Celestial Mechanics and Dynanical Astronomy* **95**, 327–344
6. Der, G., (2012). New Angles-only Algorithms for Initial Orbit Determination. *Advanced Maui Optical and Space Surveillance Technologies Conference*
7. Der, G., (2012). New Angles-only Algorithms for Initial Orbit Determination. *Advanced Maui Optical and Space Surveillance Technologies Conference*

8. Der, G., (2012). The Superior Lambert Algorithm. *Advanced Maui Optical and Space Surveillance Technologies Conference*

9. Frueh, C., (2019). AAE590 Space Traffic Management, Purdue University. *Course script*

10. Frueh, C., Fielder, H., Herzog, J.,(2018). Realistic Sensor Tasking Strategies. *Advanced Maui Optical and Space Surveillance Technologies Conference*

11. Frueh, C., Fielder, H., Herzog, J.,(2018). Heuristic and Optimized Sensor Tasking Observation Strategies with Exemplification for Geosynchronous Objects. *Journal of Guidance, Control, and Dynamics* **41**

12. Gooding, R., (1993). A New Procedure for Orbit Determination Based on Three Lines of Sight (Angles Only). DRA/RAE Technical Report 93004.

13. Gooding, R., (1996). A New Prcoedure for the Solution of the Classical Problem of Minimal Orbit Determination from Three Lines of Sight. *Celestial Mechanics and Dynanical Astronomy* **66**, 387–423

14. Gooding, R., (1988). On the Solution of Lambert's Orbital Boundary-Value Problem. Technical Report.

15. Kuznetsov, V., (2019). Revisiting the Determination of a Preliminary Orbit for a Celestial Body. *Solar System Research* **53**, 462-472

16. Schaeperkoetter, A., (2011). A Comprehnsive Comparison Between Angles-Only Initial Orbit Determination Techniques. *Master of Science Thesis*

17. Schumacher, P., Sabol, C., Higginson, C., Alfriend, K., (2018). Uncertain Lambert Problem. *Journal of Guidance, Control, and Dynamics* **38**, 1-2

18. Stoker, K., et al. (2020). Angles-Only Orbit Determination Accuracies with Limited Observational Arc. *Advanced Maui Optical and Space Surveillance Technologies Conference*

19. Vallado, D., (2009). Evaluating Gooding Angles-only Orbit Determination of Space Based Space Surveillance Measurements.

20. Weisman, R., Majji, M., Alfriend, K., (2014). Analytic Characterization of Measurement Uncertainty and Initial Orbit Determination on Orbital Element Representations. *Celestial Mechanics and Dynanical Astronomy* **118**, 165–195

21. Wie, B., Ahn, J., (2017). On Selecting the Correct Root of Angles-Only Initial Orbit Determination Equations of Lagrange, Laplace, and Gauss. *The Journal of the Astronautical Sciences* **64**, 50–71

8. APPENDIX

On the next two pages are tables detailing the minimum, median and maximum error of the two methods in each of the cases. The first table details quantities corresponding to the magnitude of the positional error in each case, including the velocity error at the given point, the spacing or change in true anomaly at that point, and the changing parameter of interest for this point, either eccentricity, semi-major axis, or observer latitude. The second table shows similar information but this time the minimum, median, and maximum are for that of the magnitude of velocity, showing the corresponding positional error as well.

8.1. Numerical Results

The numerical results are shown in Tabs. 4 and 5 on the next two pages.

Table 4. A table of the minimum, median, and maximum positional error for each method for each case. Also listed are the spacings and specific parameters of each of the cases and the corresponding velocity or position error. All positional parameters are given in km, velocity in km/s, spacing is in minutes, and angular quantities are in degrees.

Method/Case	Quantity	Minimum	Median	Maximum
Gauss Eccentricity	r_{error}	60.1560	3.3039e+04	1.9196e+07
	v_{error}	0.0117	2.4928	1.2403e+03
	$Spacing$	64.0526	316.2632	316.2632
	e	0.1056	0.9500	0
Gauss SMA	r_{error}	107.5519	6.5589e+04	5.1780e+06
	v_{error}	0.1962	5.0151	235.1818
	$\Delta TrueAnomaly$	14.2648	270	113.7174
	SMA	6778	4.2164e+04	4.2164e+04
Gauss Observer Latitude	r_{error}	83.9877	9.4717e+04	2.3268e+06
	v_{error}	0.0288	5.2930	105.9556
	$\Delta TrueAnomaly$	9.6227	181.8000	114.8422
	$ObserverLatitude$	80	90	10
Gooding Eccentricity	r_{error}	5.5042	64.6592	9.6726e+08
	v_{error}	4.4967e-04	0.0024	3.6769e+04
	$Spacing$	410.8421	600	536.9474
	e	0.1056	0.9500	0.1056
Gooding SMA	r_{error}	0.3182	1.5319e+04	2.4637e+19
	v_{error}	9.9214e-04	12.7795	9.9678e+14
	$\Delta TrueAnomaly$	19.1881	0.0573	172.2346
	SMA	6778	6778	3.4301e+04
Gooding Observer Latitude	r_{error}	3.3820	39.9010	4.0824e+08
	v_{error}	2.9242e-04	0.6736	1.6790e+04
	$\Delta TrueAnomaly$	67.0151	181.8000	124.4076
	$ObserverLatitude$	60	90	0
Gooding-Der Eccentricity	r_{error}	3.5694	173.6510	9.6726e+08
	v_{error}	0.0075	NaN	5.2876e+03
	$Spacing$	316.2632	1	505.4211
	e	0.7389	NaN	0.3167
Gooding-Der SMA	r_{error}	0.3182	4.9896e+03	1.8705e+08
	v_{error}	9.9248e-04	12.7795	4.0728e+04
	$\Delta TrueAnomaly$	19.1881	0.0573	114.8422
	SMA	6778	6778	1.4642e+04
Gooding-Der Observer Latitude	r_{error}	3.6152	89.0946	1.6733e+08
	v_{error}	0.0019	NaN	5.9638e+03
	$\Delta TrueAnomaly$	124.4076	0.0573	143.5384
	$ObserverLatitude$	70	NaN	80

Table 5. A table of the minimum, median, and maximum velocity error for each method for each case. Also listed are the spacings and specific parameters of each of the cases and the corresponding velocity or position error. Positional parameters are given in km, velocity in km/s, spacing is in minutes, and angular quantities are in degrees.

Method/Case	Quantity	Minimum	Median	Maximum
Gauss Eccentricity	v_{error}	0.0117	2.8713	1.2403e+03
	r_{error}	60.1560	7.8831e+04	1.9196e+07
	$Spacing$	64.0526	505.4211	316.2632
	e	0.1056	0.9500	0
Gauss SMA	v_{error}	0.0301	9.2777	293.8956
	r_{error}	430.8699	6.5948e+04	2.5213e+06
	$\Delta TrueAnomaly$	14.2648	270	113.7174
	SMA	4.2164e+04	4.2164e+04	2.2505e+04
Gauss Observer Latitude	v_{error}	0.0249	5.5046	3.0414e+05
	r_{error}	338.6655	9.7955e+04	7.6845e+04
	$\Delta TrueAnomaly$	9.6227	181.8000	38.3189
	$ObserverLatitude$	50	90	10
Gooding Eccentricity	v_{error}	4.1331e-04	0.0044	3.6879e+04
	r_{error}	5.6744	54.4320	9.1318e+08
	$Spacing$	379.3158	600	505.4211
	e	0.1056	0.9500	0.1056
Gooding SMA	v_{error}	2.7945e-04	5.5253	1.4179e+15
	r_{error}	3.5571	6.0239e+03	2.5635e+18
	$\Delta TrueAnomaly$	124.4076	0.0573	143.5384
	SMA	4.2164e+04	6778	6778
Gooding Observer Latitude	v_{error}	2.9242e-04	0.0033	1.6790e+04
	r_{error}	3.3820	1.0258e+04	4.0824e+08
	$\Delta TrueAnomaly$	67.0151	181.8000	124.4076
	$ObserverLatitude$	60	90	0
Gooding-Der Eccentricity	v_{error}	4.1331e-04	0.0131	1.0184e+04
	r_{error}	9.1363e+07	NaN	3.1958e+07
	$Spacing$	410.8421	1	64.0526
	e	0.7389	NaN	0.8444
Gooding-Der SMA	v_{error}	2.7945e-04	1.3657	3.7184e+05
	r_{error}	3.5571	6.0240e+03	1.6238e+06
	$\Delta TrueAnomaly$	124.4076	0.0573	0.0573
	SMA	4.2164e+04	6778	2.2505e+04
Gooding-Der Observer Latitude	v_{error}	2.6908e-04	0.0088	3.2828e+04
	r_{error}	0.0023	NaN	6.0675e+05
	$\Delta TrueAnomaly$	124.4076	0.0573	0.0573
	$ObserverLatitude$	70	NaN	70